Heterojunction Engineering of CdTe and CdSe Quantum Dots on TiO_2 Nanotube Arrays: Intricate Effects of Size-Dependency and Interfacial Contact on Photoconversion Efficiencies

Haihua Yang, Wenguang Fan, Aleksandar Vaneski, Andrei S. Susha, Wey Yang Teoh, and Andrey L. Rogach*

The quality of heterojunctions at the quantum dot (QD)-TiO_2 nanotube (TNT) interface has important implications on the efficiencies of photoelectrochemical solar cells. Here, it is shown that electrophoretic deposition of pre-synthesized thioacid-capped CdTe QDs results in relatively poor charge transfer across the heterojunctions. This is likely due to the intermediate layer of bifunctional linkers (S-R-COOH) in between the QDs and TNT. On the other hand, CdTe QD-sensitized TNT prepared by in situ deposition in aqueous medium provides direct QD-TNT contact, and hence more favorable heterojunction for charge transfer. This is exemplified not only by the drastic improvement in photocurrent efficiencies, but also provides clear difference on the size-dependent electron injection efficiencies from the CdTe QDs of different sizes. By extending the system further to CdSe QDs, drastic enhancement is found when carrying out the *in situ* deposition in an organic medium. The results are discussed in terms of the nature of deposition and the corresponding charge transport characteristics. More importantly, the work reflects the intricacy of the effects of QD size and the quality of the heterojunctions on the overall photoconversion efficiencies.

1. Introduction

Chemical photovoltaic conversion has attracted much interest in the last two decades as an attractive low-cost alternative to the silicon-based solar cells. Although initial efforts were predominantly focused on the dye-sensitized or Grätzel-type solar cells,[1–3] the last decade has seen variants of other architectures, for example, organic[4] and quantum dot (QD)-sensitized ones.[5] With much progress in the research on colloidal nanocrystal QDs,[6] their application in solar cells is in particular gaining momentum.[7–10]

The excellent tunability of the optoelectronic properties of QDs has become one of the most attractive properties in its design, allowing their harnessing of low energy solar photons.[11] This can be achieved by facile modification of the size of QDs and their resulting band structures through the size quantization effect. Of equal importance is the manipulation of charge transport properties of these QDs that allows efficient interfacial transfer of the electron-hole pair. This is particularly important in QD-sensitized solar cells (QDSSCs), where the interfacing with wide bandgap semiconductor nanostructures, such as TiO_2 and ZnO, affects the overall net photovoltaic efficiencies.[7] Alignment of QD band structures with that of the wide bandgap semiconductor has intriguing effects on the interfacial charge transport efficiencies. To date, although a wide range of QDs, from CdSe, CdS, CdTe, PbS to PbSe, has been utilized in QDSSCs,[10] their effects on charge transport deserve more in-depth understanding.

In the current work, we demonstrate the impact of interfacing CdTe and CdSe QDs of different physicochemical characteristics with aligned TiO_2 nanotube arrays (TNT). The high density of states of TiO_2 conduction band enables its function as one of most suitable electrons acceptor,[12] while the one-dimensional (1-D) alignment was considered to be favourable for the vectorial charge transport.[13–16] By devising novel techniques of synthesis and interfacing of QDs on TNT, meaningful insights on the charge transport can be obtained further enabling a multiple-fold increase in photovoltaic efficiencies. Besides photovoltaic conversion, this work has further implications to the wider photoelectrochemical and photocatalytic applications, e.g., water splitting[17] and CO_2 reduction,[18] where the existence of QD-photocatalyst heterojunction is concerned.

W. Fan, Dr. W. Y. Teoh
Clean Energy and Nanotechnology (CLEAN) Laboratory
School of Energy and Environment
City University of Hong Kong
Shatin, N. T., Hong Kong SAR
E-mail: wyteoh@cityu.edu.hk

H. Yang, A. Vaneski, Dr. A. S. Susha, Prof. A. L. Rogach
Department of Physics and Materials Science
and Centre for Functional Photonics (CFP)
City University of Hong Kong
Tat Chee Avenue, Kowloon, Hong Kong SAR

DOI: 10.1002/adfm.201103074

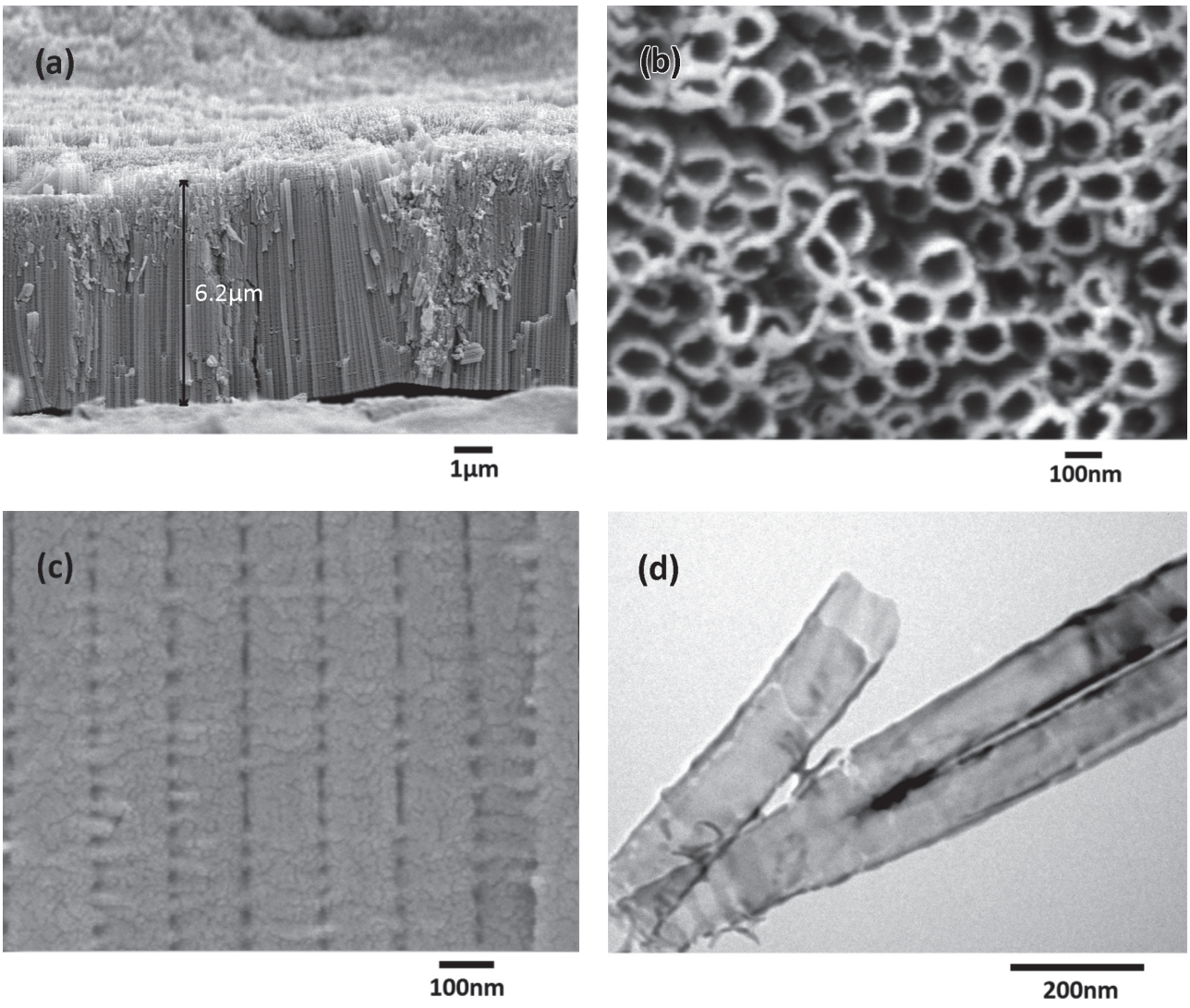

Figure 1. FE-SEM images of the anodized TNT annealed at 773 K for 6 h: a) cross-section, b) top view, c) cross-section zoom in, and d) TEM images of single nanotube array.

2. Results and Discussion

2.1. Fabrication of Titania Nanotube Arrays

TNT arrays are fabricated by a recently reported etching anodization of titanium foil using sodium fluoride as the complexation etching source, instead of the more toxic hydrofluoric acid or ammonium fluoride.[19] Prior to the decoration with QD, the bare TNT arrays were parametrically optimized to display the highest photocurrent efficiency, which could be achieved by anodization at 40 V and 12 h (see Supporting Information, Figure S2). As shown from the analysis by field emission-scanning electron microscopy (FE-SEM) in **Figure 1**, the TNT arrays consisted of vertically aligned TNT bundles of 6.2 μm in length and average pore diameter of 80 nm. In its bare form, decreased photocurrent was measured at higher applied voltage and longer anodisation duration than the optimal condition due to the bundling of tubes at higher aspect ratios (Figure S3, Supporting Information). As shown in Figure 1c, the tubes consist of relatively smooth wall (~20 nm thick) with only slight ripples evident on the exterior wall. In general, the extent of ripples is a function of electrolyte viscosity and water content, where rough surfaces were reported at high water content, likely due to the periodic current fluctuation and the resulting diffusion of fluoride etching ions during the anodization process.[19,20] At 5% water content in ethylene glycol, we maintained both the solubility of sodium fluoride salts and smoothness of the TNT surface.

Analysis of the TNT by X-ray diffraction (Figure S1, Supporting Information) and further Rietveld refinement found predominantly anatase content with only trace amount of rutile (<0.5 mol%) after annealing at 773 K. Although pure anatase phase could be obtained by annealing at 673 K instead of 773 K, we found higher photoconversion efficiencies in the latter. Difference is noted between the present work and that reported by Zhu et al.,[21] who reported optimal photovoltaic conversion for

N719 dye-sensitized TNT array annealed at 673 K. The difference reflects the nature of substrate- and electrolyte-dependence of TNT in terms of its charge transport properties. The presence of rutile creates polymorphic heterojunctions which potentially enhances the charge separation along the polycrystalline TiO_2.[22] Annealing at higher temperatures promoted higher degree of anatase-to-rutile phase transformation and accompanying deformation of the vertically-aligned nanotubes structure.

2.2. Sensitization of TNT with CdTe QDs by Electrophoretic Deposition and *In Situ* Deposition

Two facile strategies of anchoring aqueous-based CdTe QDs onto TNT arrays were explored in this study, providing means of variability in the deposition characteristics. They are the (i) electrophoretic deposition (EPD) technique and (ii) *in situ* deposition of QDs. During EPD, conjugation of pre-synthesized, thioacid-capped colloidal QDs on surface titanol through the carboxyl moiety is established. CdTe QDs of two different sizes, 2.4 and 3.1 nm, both capped with mercaptoproprionic acid, were obtained as reported previously.[23] The difference in the QD size is clearly reflected by the blue shift in the absorption threshold of the smaller size CdTe QD (Figure S4, Supporting Information). The size quantization of CdTe QD results in the shifting of conduction band to a more negative level, which as will be shown later, is beneficial to the charge separation and interfacial electrons transfer across the QD-TNT heterojunction.

The voltage applied during the EPD provided external driving force for which colloidal QDs could approach the TNT electrode surface. By increasing the applied potential from +2.0 to +5.0 V, the amount of conjugated CdTe QDs on TNT array could be improved by up to 3-fold (in the case of CdTe QDs of 3.1 nm in size, **Table 1**). The EPD technique was essentially limited by the electrolysis of water at applied potential higher than +5.0 V, resulting in the formation of gaseous H_2 and O_2 on electrode surface that prevented QDs from approaching TNT electrode surface. (Note: the applied potential is higher than the theoretical +1.23 V for electrochemical water splitting, as a result of overpotential). Non-specifically attached QDs were removed by thorough rinsing with deionized water after the EPD.

Table 1. Element concentration and number (*N*) of QDs on TNT per working electrode area. Concentrations were determined by ICP–AES, with accuracies Cd: 0.5%; Se: 2.0%; Te: 1.5%.

	Cd [mol cm^{-2}]	Se [mol cm^{-2}]	Te [mol cm^{-2}]	*N* [cm^{-2}]
TNT-CdTe (2.4 nm), EPD +2.0 V	2.03×10^{-8}	–	1.78×10^{-8}	9.5×10^{13}
TNT-CdTe (2.4 nm), EPD +5.0 V	6.43×10^{-8}	–	5.65×10^{-8}	3.0×10^{14}
TNT-CdTe (3.1 nm), EPD +2.0 V	1.36×10^{-8}	–	1.14×10^{-8}	2.8×10^{13}
TNT-CdTe (3.1 nm), EPD +5.0 V	4.13×10^{-8}	–	3.52×10^{-8}	8.7×10^{13}
TNT-CdTe (2.3 nm), *in situ* aqueous	4.86×10^{-8}	–	3.63×10^{-8}	2.2×10^{14}
TNT-CdTe (3.1 nm), *in situ* aqueous	5.07×10^{-8}	–	3.72×10^{-8}	9.3×10^{13}
TNT-CdSe (2.2 nm), *in situ* aqueous	1.46×10^{-7}	1.04×10^{-7}	–	6.1×10^{14}
TNT-CdSe (6.9 nm), *in situ* organic	6.75×10^{-7}	5.77×10^{-7}	–	1.1×10^{14}

In the *in situ* deposition approach, bare TNT electrode was introduced in the reaction medium for which the QDs were synthesized.[24] Despite the presence of an external nucleation site, i.e. TNT surface, little difference in terms of the size of product QDs was observed with and without TNT (Figure S4, Supporting Information). The initial coordination of Cd^{2+} with $Ti\text{-}O^-$ was thought to be the nucleation site for which QDs to grow on. While the amount of QDs are comparable to that deposited by EPD technique at the higher voltage (Table 1), as we show below, the nature of QDs interfacing achieved during the *in situ* deposition is particularly advantageous for the efficient photoelectron transfer.

Studies on the photoelectrochemical properties of the QD-sensitized TNT were carried out in a standard three-electrode cell. Here, the bare TNT arrays and CdTe QDs were confirmed to be of n-type nature (Figure S5, Supporting Information). Typical anodic photocurrents were observed for the CdTe QD-sensitized TNT under full arc as well as $\lambda > 455$ nm irradiation. As shown in **Figure 2**a, significant increase in photocurrent by 5 and 6 folds, under full arc irradiation could be obtained by electrophoretic deposition (EPD voltage +5.0 V) of CdTe QDs with size of 3.1 and 2.4 nm, respectively, on the TNT arrays. Under the irradiation of $\lambda > 455$ nm where TiO_2 cannot be excited, we continue to observe photocurrent solely by injection from the CdTe QDs (Figure 2c), which difference in photocurrent was within the range expected from the difference in CdTe density (Table 1). Note the lower absolute photocurrent under $\lambda > 455$ nm compared to full arc irradiation is predominantly due to the filling of sub-bandgap states, that is, defects of TNT, upon injection of photoelectrons from the QDs.

A marked improvement in photocurrent is observed for CdTe QD-sensitized TNT prepared by *in situ* deposition (Figure 2b), compared to that deposited by the EPD. This is true despite similar CdTe nanocrystals density in both cases at the comparable QD sizes (Table 1). In such case, the enhanced photocurrent for the *in situ* deposited sample is most likely to stem from the more favorable interfacial contact, since the QDs were grafted and grown directly onto the TNT surface site. Like that prepared by EPD, CdTe QDs of smaller size displays higher photocurrent response (12 folds relative to bare TNT) than that of the larger size (5 folds relative to bare TNT). Important experimental evidence could be drawn from the current set of results, which shows that despite fractional increase (30%) in QDs density in the 2.3 nm CdTe QDs compared to that of 3.1 nm, photocurrent could be enhanced by as much as ~2.4 fold under full arc irradiation. As discussed by Kamat and coworkers,[25,26] the more negative conduction band-edge of smaller QDs favours faster interfacial electrons injection in the Marcus normal region,[27] resulting in higher measured photocurrent. Here, the difference in conduction band-edges of the two different sizes of CdTe QDs was estimated to be approximately 0.1 eV.[28] Similar extent of quantisation-induced photocurrent enhancement could not however be observed for the EPD prepared samples, stressing the importance of the quality of the

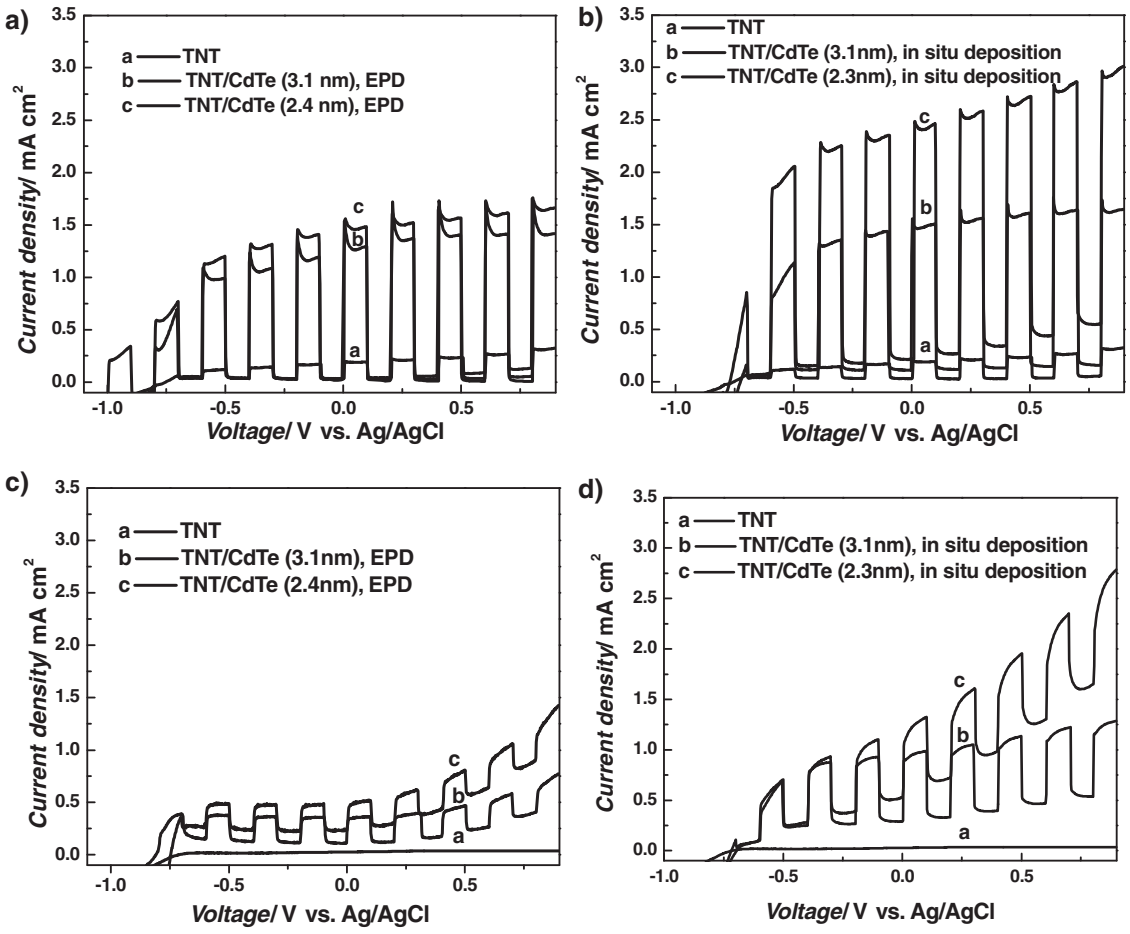

Figure 2. Photocurrent response (in chopping mode, light on-off repeatedly) of bare TNT and that sensitized with CdTe QDs deposited by EPD under a) full arc and c) $\lambda > 455$ nm. Also shown are the corresponding samples prepared by *in situ* deposition by aqueous synthesis under b) full arc and d) $\lambda > 455$ nm irradiation.

QD-TNT heterojunctions (**Scheme 1**). It is further noted that only incremental enhancement related to the CdTe QDs density was measured at $\lambda > 455$ nm when the TNT was not photoexcited, implying synergistic effect when both TNT and QDs are excited. Detailed fundamental studies are currently being devoted to understand this effect.

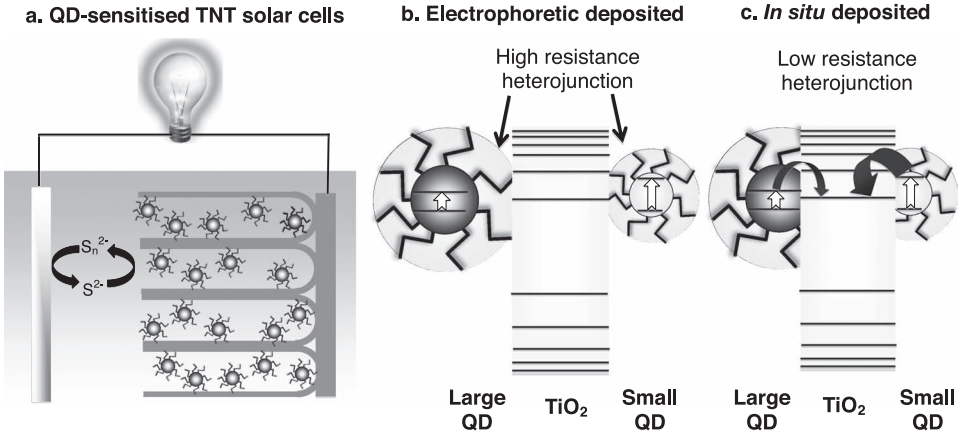

Scheme 1. a) An illustration of the QD-sensitized TNT photoelectrochemical solar cells used in the current study. Also shown are the schematic illustrations of the nature of heterojunctions formed by QDs by b) EPD and c) *in situ* deposition. The more negative conduction band-edge in smaller size QD resulted in efficient interfacial electron injection across the low resistance heterojunction.

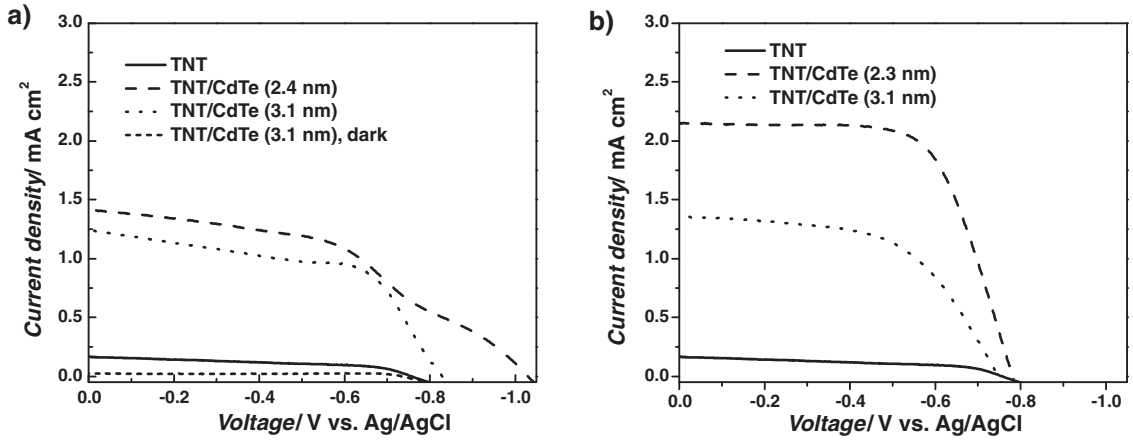

Figure 3. *I–V* curves of bare TNT and that sensitized by CdTe QDs of different sizes deposited by a) EPD under +5.0 V, and b) *in situ* deposition by aqueous synthesis. Light source: 300 W xenon lamp.

Figure 3 shows the typical *I–V* curves of the CdTe QD-sensitized TNT prepared by both the EPD and in situ deposition. It is evident that there are at least two intangible factors that result in the increase in the open circuit voltages (V_{OC}), or the difference between the Fermi level of the photoanode (QD-sensitized TNT) and equilibrated redox (S^{2-}/S_n^{2-}) potential at the counter electrode.[9,30] The first being the higher density of QDs on TNT, and second, the more negative conduction band edge of smaller size QDs. As discussed above, both factors result in the higher rates of photoelectrons injection. Essentially, the higher rates of photoelectrons injection (as reflected by the net short-circuit current, J_{SC}) are almost synonymous to the more negative shift in photoanode Fermi level, i.e., higher V_{OC} (**Table 2**).

To gain more in-depth understanding on the charge transport properties, the electron lifetime (τ_e) of QD-sensitized TNT was measured as a function of the rate of V_{OC} decay.[15,30] Under continuous irradiation, steady state exists between all charge transport processes, including the forward electron injection from QDs to TNT, hole scavenging by S^{2-}, and recombination of accumulated electrons with the oxidized form of the redox couple (S_n^{2-}).[29] This results in a steady open circuit potential as shown in **Figure 4**. Upon termination of excitation source, recombination of accumulated electrons with oxidized form of redox couple (S_n^{2-}) and photoholes dominates, resulting in the decay of V_{OC}. At comparable V_{OC}, TNT sensitized with 2.4 nm CdTe QDs (by EPD) displays a magnitude higher in electron lifetime compared to the bare TNT (Figure 4b). It is hypothesized the photoelectrons are trapped at the QD-TNT heterojunction thereby suppressing its rapid recombination with S_n^{2-}. This is consistent with our earlier discussion that the heterojunction between electrophorectic deposited QDs and TNT may be the limiting interface for efficient electron transfer.

Table 2. Characteristics of open circuit voltage (V_{OC}) and short circuit current (J_{SC}) of bare TNT and TNT sensitized with CdTe and CdSe QDs by various deposition conditions. Light source: Full arc 300 W xenon lamp; Counter electrode: Pt; Electrolyte: Aqueous-based 0.1 M Na_2S and 0.01 M sulfur.

QDs [nm]	V_{oc} [V vs Ag/AgCl]	J_{sc} [mA cm^{-2}]
Bare TNT	0.76	0.17 ± 0.01
TNT-CdTe 2.4 nm (EPD +2.0 V)	0.99	0.87 ± 0.03
TNT-CdTe 2.4 nm (EPD +5.0 V)	1.03	1.42 ± 0.04
TNT-CdTe 3.1 nm (EPD +2.0 V)	0.80	0.80 ± 0.02
TNT-CdTe 3.1 nm (EPD +5.0 V)	0.83	1.25 ± 0.03
TNT-CdTe 2.3 nm (*in situ* deposition, aqueous)	0.78	2.15 ± 0.05
TNT-CdTe 3.1 nm (*in situ* deposition, aqueous)	0.75	1.14 ± 0.02
TNT-CdSe 2.2 nm (*in situ* deposition, aqueous)	1.23	3.12 ± 0.04
TNT-CdSe 6.9 nm (*in situ* deposition, organic)	0.78	1.58 ± 0.02

The difference in the nature of QD-TNT interfacial contact between EPD and that of *in situ* deposition is further exemplified by the electron lifetime measurements of the latter (Figure 4d). Compared to that of EPD, the direct growth of CdTe on TNT during *in situ* deposition resulted in more intimate interfacial contact, and hence of lower resistance (Scheme 1). In other words, the trapping of electrons at the heterojunction is less efficient. For this reason, variability in electron lifetime is less significant between samples with and without QD-sensitisation. In fact, the more efficient electron injection from the conduction band of 2.4 nm CdTe QDs to that of TNT, may have resulted in shorter lifetime as a result of recombination with photoholes and/or S_n^{2-}. Enhanced recombination of conduction band electrons from TNT with the photoholes at the now more positive CdTe valence band edge is also possible in this case.

2.3. Sensitization of TNT with CdSe QDs by *In Situ* Deposition from Aqueous and Organic Phase

Studies on QD-sensitized TNT were further extended to the CdSe QD systems. Perhaps more differently, comparisons between *in situ* deposition of CdSe QDs on TNT were carried out in aqueous as well as organic phase. The latter is a well-established technique for the preparation of a wide range of

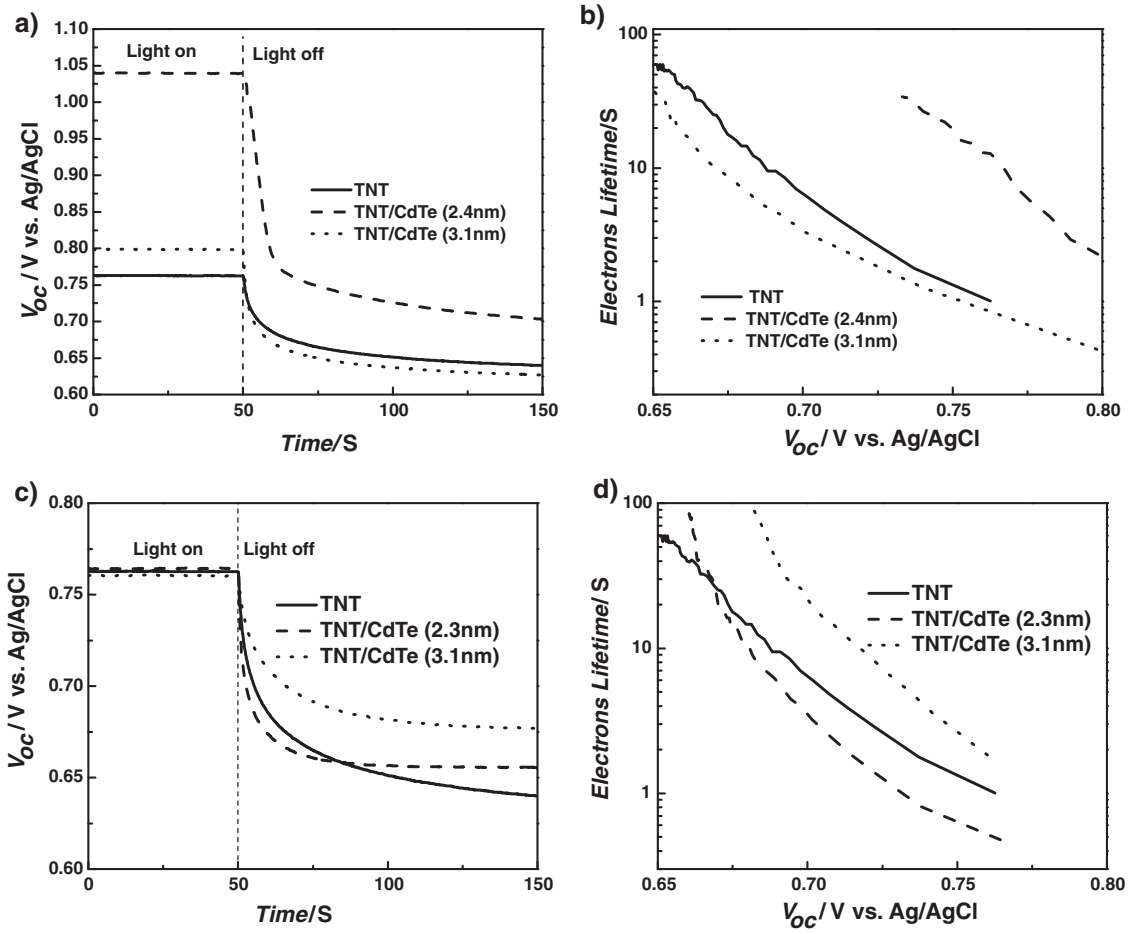

Figure 4. a) Profiles of V_{oc} decay of bare TNT and that sensitized by CdTe QD of different sizes by EPD under +5.0 V, as well as the corresponding electron lifetimes as a function of V_{oc}. Also shown are the V_{oc} decay profiles of CdTe QD-sensitized TNT prepared by *in situ* deposition by aqueous synthesis, and the corresponding electron lifetimes as a function of V_{oc}.

colloidal QDs, as previously reported by us as well as others.[31–33] **Figure 5**a shows the absorption spectra of the CdSe QDs as-synthesized in the aqueous and organic phases. The CdSe particle sizes were determined to be 2.2 and 6.9 nm, respectively.[34] It is worth noting that the particle growth rate of CdSe QDs in the organic medium was accelerated greatly by the introduction of TNT arrays. The absence of steric hydration layer in organic medium provided more sites for which Cd^{2+} could conjugate with Ti-O^{-}. As a result of the close proximity of the nucleation sites, the formed CdSe nanoparticles are prone to higher growth rates by surface coalescence. Figures 5b and c show homogeneous dispersion and high crystallinity of CdSe QDs on TNT. High density of CdSe QDs on TNT was obtained by the *in situ* deposition, in the same order of magnitudes as that for CdTe QDs (Table 1). Near stoichiometric Cd:Se ratio of 1:1 were obtained in all cases, as confirmed by X-ray photoelectron spectroscopy and inductively-coupled plasma–atomic emission spectroscopy elemental analyses. Perhaps due to the more prevalent surface coalescence during *in situ* deposition of CdSe QDs in organic medium, the density of QDs nanocrystals was 6 times less than that deposited in aqueous medium.

As shown in **Figure 6**a, a remarkable 18 fold increase in photocurrent relative to bare TNT was obtained for the electrode prepared by *in situ* deposition of CdSe QDs in organic medium. This is twice that of CdSe QD-sensitized TNT electrode synthesized in aqueous medium, despite its much larger crystal size and lower QD density. As further shown in the *I–V* curves in Figure 6b, the high photoelectron density in the organics-prepared sample was accompanied by the significant enhancement in V_{OC} (highest in the current study) as compared to the bare TNT and that *in situ* sensitized in aqueous medium (Table 2). Again, this is true despite the much lower conduction band edge of the large CdSe QDs; difference between that of 2.2 and 6.9 nm estimated to be >0.2 eV.[39] At first glance, this may appear to contradict Marcus theory and the earlier work by Kamat and coworkers on the CdSe QD-TiO_2 system.[25] However, meaningful insights could be obtained from the electron lifetime as discussed below.

As shown in Figure 6c, a magnitude increase in electron lifetime was measured for the sample sensitized with 6.9 nm CdSe QDs in organic medium, relative to that of bare TNT as well as that in situ sensitized in aqueous medium. Based on our earlier hypothesis that more favorable QD-TNT interfacial contact formed during *in situ* deposition, one would expect the smaller size aqueous-synthesized CdSe QDs to be more efficient in transferring photoelectrons across the QD-TNT heterojunction

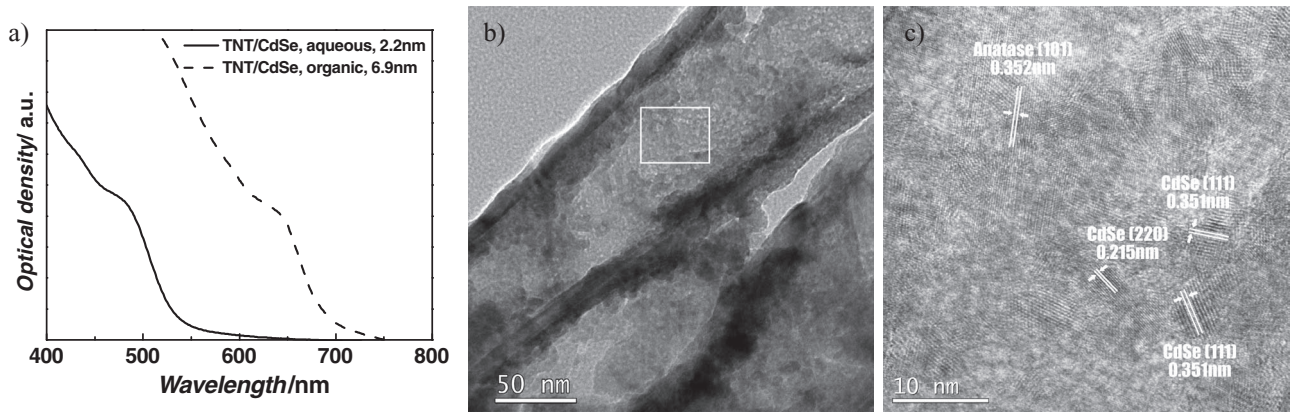

Figure 5. a) UV–vis absorption spectra of CdSe QDs synthesized during the *in situ* deposition in aqueous and that in organic medium. Note the significant blue shift in absorption threshold as a result of smaller size CdSe QDs. b) TEM image and the corresponding c) HRTEM of CdSe QD-sensitized TNT prepared by in situ deposition in organic medium.

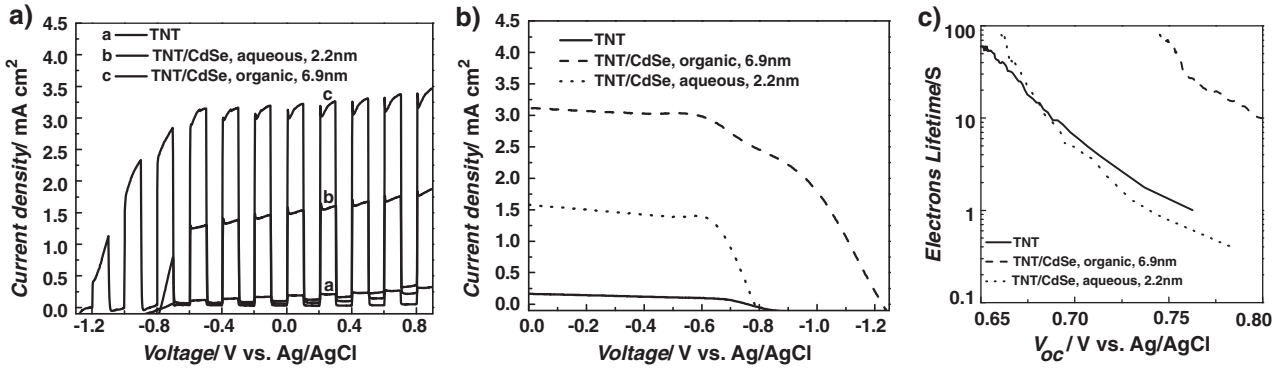

Figure 6. a) Photocurrent response of bare TNT and that sensitized by CdSe QDs prepared by *in situ* deposition in aqueous and organic medium. Also shown are the corresponding b) *I–V* curves, and c) electrons lifetime as a function of V_{OC}.

and undergo rapid recombination. In fact, the electron lifetime profile matches closely that of bare TNT, suggesting rapid and efficient injection of photoelectrons across the interface. By contrast, there exists smaller driving force in the larger size organic-synthesized CdSe for such interfacial electron migration and recombination. At the same time, its less positive valence band edge would also minimize the driving force for photoholes recombination with TiO_2 conduction band electrons. These factors resulted in longer electron lifetime of the organic-synthesized CdSe-TNT. Furthermore, the surface recombination of S_n^{2-} and photoelectrons as a function of QDs surface area (inversely proportional to size), relative to charge injection, is an interesting possibility that deserves detailed kinetic studies.

3. Conclusions

The quality of heterojunctions established through the deposition of CdTe and CdSe QDs on TNT has important impacts on the overall photoconversion efficiencies. In particular, we show in this work that electrophoretic deposition of pre-synthesized thioacid-capped QDs resulted in heterojunctions that may have limited the photoelectrons transfer efficiencies across the QD-TNT interface. By comparison, QDs that were *in situ* synthesized and deposited onto TNT (i.e.; direct grafting) show much favorable interfacial charge transfer. By establishing such favorable contact, the effect of size-dependent electron injection efficiencies of different sizes QDs became apparent (Marcus theory). As a result, enhancement in photocurrent up to 18 fold for CdSe QD-sensitized TNT was measured, relative to that of bare TNT. Besides photoconversion, the findings from this work have important implications on the wider applications such as sensors, photocatalysis and nanoelectronics, where charge transfer across QD-metal oxide heterojunctions is critical. In fact, the work may have fundamental importance to the extraction of multiple excitons or hot carriers in third generation solar cells.

4. Experimental Section

Fabrication of Titanium Nanotube (TNT) Arrays: Fabrication of TNT arrays by anodization is similar to that reported by Yun et al.[19] The electrolyte composed of 0.5 wt.% sodium fluoride (Acros Organics, 99+%), 5 wt.% milli-Q water, and 94.5 wt.% ethylene glycol (Sigma Aldrich, 99%). The titanium foil (Strem Chemicals, 99.7%) was mounted in a Teflon cell as the anode, with a platinum foil as the counter cathode. The anodization was carried out at 40 V for 12 h. The anodized foil was annealed at 500 °C for 6 h with the ramping rate of 5 °C min^{-1} in air.

Aqueous Synthesis and In Situ Deposition of CdTe QDs and CdSe QDs onto TNT: The CdTe and CdSe QD capped by a short-chain ligand mercaptopropionic acid (MPA) were synthesized in water as reported previously.[23,35] Cadmium perchlorate ($Cd(ClO_4)_2$, 2.35 mmol) was dissolved in 500 mL and 125 mL of water, for CdTe QDs and CdSe QDs, respectively. MPA (5.74 mmol) was added under vigorous stirring, followed by adjusting the pH value to 11.2 by dropwise addition of 1 M solution of NaOH. The mixture was deaerated by argon bubbling for 30 min, and 5.9 mL of fresh NaHTe or NaHSe solution (0.1 M) was injected into the mixture, followed by heating and maintaining boiling until getting CdTe QDs or CdSe QDs with desired size by monitoring UV–vis absorption spectra. For in situ deposition of CdTe QDs or CdSe QDs onto TNT, TNT substrate was placed into cadmium precursor and stirred for 30 mins before the injection of tellurium precursor or selenium precursor. The TNT sample was taken out when getting CdTe QDs or CdSe QDs with desired size by monitoring UV–vis absorption spectra.

Organic Synthesis and In Situ Deposition of CdSe QDs onto TNT: An amount of 0.42 g (1.58 mmol) of cadmium acetate ($Cd(CH_3COO)_2$), 5.56 g (23.03 mmol) of n-hexadecylamine (HDA), 1.35 g (5.41 mmol) dodecyl phosphonic acid were heated to 80 °C and degassed by vacuum using Schlenk line technique. TNT substrate was placed into precursor solution, which was heated while stirred under nitrogen atmosphere to 270°C. At this temperature a solution of readily dissolved and degassed 0.4 g of selenium in 8 g trioctylphosphine (TOP) were quickly injected using a syringe. The reaction was quenched by removing the heating mantle and the mixture was allowed to cool down.

Electrophoretic Deposition (EPD) of CdTe QDs onto TNT: The as-obtained CdTe QDs with negative charges are capped with MPA, which is a bifunctional linker molecules (HOOC-R-SH). Carboxylate group of the ligand has good affinity for TiO_2, which enables the binding of CdTe QDs to TNT.[36,37] Here we utilize EPD to facilitate the transport and binding of CdTe QDs to TNT anode. The EPD cell was filled with 13 mL water, and constructed to a two-electrode system, comprising of TNT anode and platinum counter electrode. By applying voltage of +2.0 and 5.0 V, 0.2 mL of CdTe QDs solution (10^{16} particles/mL) was added every 5 min for 10 times under magnetic stirring. The total duration of EPD was 2 hours.

Characterization: X-ray diffraction (XRD) was carried out on Bruker D8 Diffractometer using Cu Kα radiation, scanning from 2θ of 10 to 100°, at 0.03°/min and 15 s per step. Quantification of the crystallite content was further analyzed by Rietveld refinement using the commercial X'Pert Highscore Plus software.[22,38] The morphology of the samples was observed with a field emission-scanning electron microscope (FE-SEM, JEOL JSM 7001F) and transmission electron microscope (TEM; a Philips CM20). High-resolution transmission electron microscope (HRTEM) images were obtained with a Philips CM200 operated at 200 kV. UV–vis absorption spectra were measured on Varian Cary 50 UV–visible spectrophotometer. Fluorescence emission spectra were recorded on a Varian (Cary Eclipse) fluorescence spectrophotometer. Element concentration on TNT was determined by inductively-coupled plasma–atomic emission spectroscopy (ICP–AES) (Perkin Elmer, Optima 2100DV). Number (N) of QDs on TNT was estimated from element concentration on TNT and QDs particle size.

PEC Measurements: The PEC set up followed a classic three-electrode system, comprising of CdTe QDs or CdSe QDs sensitized TNT photoanode, platinum counter electrode and Ag/AgCl reference electrode. The electrolyte consists of 0.1 M Na_2S and 0.01 M sulfur aqueous solution deaerated with N_2 for 30 min prior to use. A 300 W xenon lamp (Newport) was used as the light source providing irradiance intensity of 0.896 W cm^{-2}. In some cases, GG455 (Schott) was used to provide $\lambda > 455$ nm. A Solartron Modulab potentiostat was employed to record the photocurrent and open-circuit voltage characteristics. The electron lifetime was deduced from the decay of open circuit voltage (V_{OC}) upon termination of irradiation:[15,30]

$$\tau_n = -\frac{k_B T}{e}\left(\frac{dV_{OC}}{dt}\right)^{-1} \quad (1)$$

Where k_B is the Boltzmann's constant, T is temperature, and e is the elementary charge.

Supporting Information

Supporting Information is available from the Wiley Online Library or from the author.

Acknowledgements

The authors thank Professor Lutz Mädler and Dr Huanjun Zhang (University of Bremen) for XRD measurements. This work was supported by GRF projects 103311 and 102810 from the Research Grants Council of Hong Kong.

Received: December 19, 2011
Revised: February 17, 2012
Published online: April 10, 2012

[1] B. O'Regan, M. Grätzel, *Nature* **1991**, *353*, 737.
[2] A. Hagfeldt, M. Grätzel, *Acc. Chem. Res.* **2000**, *33*, 269.
[3] M. Grätzel, *Acc. Chem. Res.* **2009**, *42*, 1788.
[4] H. Imahori, T. Umeyama, *J. Phys. Chem. C* **2009**, *113*, 9029.
[5] P. V. Kamat, K. Tvrdy, D. R. Baker, J. G. Radich, *Chem. Rev.* **2010**, *110*, 6664.
[6] A. L. Rogach, Ed. Semiconductor*Nanocrystal Quantum Dots,* Springer, New York **2008**
[7] P. V. Kamat, *J. Phys. Chem. C* **2008**, *112*, 18737.
[8] I. Mora-Seroó, J. Bisquert, *J. Phys. Chem. Lett.* **2010**, *1*, 3046.
[9] S. Ruhle, M. Shalom, A. Zaban, *ChemPhysChem* **2010**, *11*, 2290.
[10] F. Hetsch, X. Xu, H. Wang, S. V. Kershaw, A. L. Rogach, *J. Phys. Chem. Lett.* **2011**, *2*, 1879.
[11] A. L. Rogach, *Nano Today* **2011**, *6*, 355.
[12] B. C. O'Regan, J. R. Durrant, *Acc. Chem. Res.* **2009**, *42*, 1799.
[13] G. K. Mor, K. Shankar, M. Paulose, O. K. Varghese, C. A. Grimes, *Nano Lett.* **2006**, *6*, 215.
[14] J. R. Jennings, A. Ghicov, L. M. Peter, P. Schmuki, A. B. Walker, *J. Am. Chem. Soc.* **2008**, *130*, 13364.
[15] J. H. Bang, P. V. Kamat, *Adv. Funct. Mater.* **2010**, *20*, 1970.
[16] J. H. Park, S. Kim, A. J. Bard, *Nano Lett.* **2006**, *6*, 24.
[17] H. M. Chen, C. K. Chen, Y.-C. Chang, C.-W. Tsai, R.-S. Liu, S.-F. Hu, W.-S. Chang, K.-H. Chen, *Angew. Chem. Int. Ed.* **2010**, *49*, 5966.
[18] C. Wang, R. L. Thompson, J. Baltrust, C. Matranga, *J. Phys. Chem. Lett.* **2010**, *1*, 48.
[19] J.-H. Yun, Y. H. Ng, C. Ye, A. J. Mozer, G. G. Wallace, R. Amal, *ACS Appl. Mater. Interfaces* **2011**, *3*, 1585.
[20] S. Li, G. Zhang, D. Guo, L. Yu, W. Zhang, *J. Phys. Chem. C* **2009**, *113*, 12759.
[21] K. Zhu, N. R. Neele, A. F. Halverson, J. Y. Kim, A. J. Frank, *J. Phys. Chem. C* **2010**, *114*, 13433.
[22] Y. K. Kho, A. Iwase, W. Y. Teoh, L. Maädler, A. Kudo, R. Amal, *J. Phys. Chem. C* **2010**, *114*, 2821.
[23] N. Gaponik, D. V. Talapin, A. L. Rogach, K. Hoppe, E. V. Shevchenko, A. Kornowski, A. Eychmuller, H. Weller, *J. Phys. Chem. B* **2002**, *106*, 7177.
[24] H. Wang, C. Luan, X. Xu, S. V. Kershaw, A. L. Rogach. *J. Phys. Chem. C.* **2012**, *116*, 484.
[25] I. Robel, M. Kuno, P. V. Kamat, *J. Am. Chem. Soc.* **2007**, *129*, 4136.
[26] K. Tvrdy, P. A. Frantsuzov, P. V. Kamat, *Proc. Natl. Acad. Sci. USA* **2011**, *108*, 29.

[27] R. A. Marcus, *J. Chem. Phys.* **1965**, *43*, 679.
[28] S. K. Haram, A. Kshirsagar, Y. D. Gujarathi, P. P. Ingole, O. A. Nene, G. B. Markad, S. P. Nanavati, *J. Phys. Chem. C* **2011**, *115*, 6243.
[29] V. Chakrapani, D. Baker, P. V. Kamat, *J. Am. Chem. Soc.* **2011**, *133*, 9607.
[30] A. Zaban, M. Greenshtein, J. Bisquert, *ChemPhysChem* **2003**, *4*, 859.
[31] D. V. Talapin, A. L. Rogach, A. Kornowski, M. Haase, H. Weller, *Nano Lett.* **2001**, *1*, 207.
[32] C. B. Murray, D. J. Norris, M. G. Bawendi, *J. Am. Chem. Soc.* **1993**, *115*, 8706.
[33] P. Reiss, J. Bleuse, A. Pron, *Nano Lett.* **2001**, *2*, 781.
[34] W. Yu, L. H. Qu, W. Z. Guo, X. G. Peng, *Chem. Mater.* **2003**, *15*, 2854
[35] A. L. Rogach, A. Kornowski, M. Gao, A. Eychmüller, H. Weller, *J. Phys. Chem. B* **1999**, *103*, 3065.
[36] X. F. Gao, H. B. Li, W. T. Sun, Q. Chen, F. Q. Tang, L. M. Peng, *J. Phys. Chem. C* **2009**, *113*, 7531.
[37] I. Robel, V. Subramanian, M. Kuno, P. V. Kamat, *J. Am. Chem. Soc.* **2006**, *128*, 2385.
[38] Y. K. Kho, W. Y. Teoh, A. Iwase, L. Mädler, A. Kudo, R. Amal, *ACS Appl. Mater. Interfaces* **2011**, *3*, 1997.
[39] S. N. Inamdar, P. P. Ingole, S. K. Haram, *ChemPhysChem* **2008**, *9*, 2574.